Available online at www.sciencedirect.com
SciVerse ScienceDirect
Journal of the European Ceramic Society xxx (2012) xxx–xxx
www.elsevier.com/locate/jeurceramsoc

Influence of countersurface materials on dry sliding performance of CuO/Y-TZP composite at 600 °C

Mahdiar Valefi [a,*], Belavendram Pathiraj [b], Matthijn de Rooij [a], Erik de Vries [a], Dirk J. Schipper [a]

[a] University of Twente, Faculty of Engineering Technology, Surface Technology and Tribology, P.O. Box 217, 7500 AE Enschede, The Netherlands
[b] University of Twente, Faculty of Engineering Technology, Applied Laser Technology, Enschede, The Netherlands

Received 13 March 2012; received in revised form 9 July 2012; accepted 14 July 2012

Abstract

Dry sliding wear tests on 5 wt.% copper oxide doped yttria stabilized zirconia polycrystals (CuO–TZP) composite have been performed against alumina, zirconia and silicon nitride countersurfaces at 600 °C. The influences of load and countersurface materials on the tribological performance of this composite have been studied. The friction and wear test results indicate a low coefficient of friction and specific wear rate for alumina and zirconia countersurfaces at $F = 1$ N load (maximum Hertzian pressure ~0.5 GPa). Examination of the worn surfaces using scanning electron microscope/energy dispersive spectroscopy confirmed the presence of copper rich layer at the edge of wear scar on the alumina and zirconia countersurfaces. However, Si_3N_4 countersurface sliding against CuO–TZP shows a relatively higher coefficient of friction and higher wear at 1 N load condition. These results suggest that the countersurface material significantly affect the behavior of the third body and self-lubricating ability of the composite.

Keywords: Y-TZP composite; Sliding wear; Tribology; Self-lubricating

1. Introduction

Sliding friction is one of the oldest problems in the field of tribology.[1,2] It can deteriorate the surface properties of engineering materials used in moving mechanical systems which have to be wear resistant under unlubricated sliding conditions. Self-lubricating composites are particularly attractive for systems where a high coefficient of friction damages the surface due to a high temperature.[3,4] Study of their self-lubricating ability under a variety of tribological conditions is of great importance.[5,6]

The self-lubricating performance of a ceramic composite depends on the incorporated solid lubricant, test conditions (such as load, sliding velocity, temperature and so on) and microstructures of mating and countersurface materials. The successful use of self-lubricating ceramic composites requires an understanding of their material properties and a knowledge of which solid lubricant formulation is best for a chosen application. Issues such as the mating counterpart material compatibility must be taken into account during the design of a lubricated device or moving mechanical assembly. Further, prediction of the coefficient of friction using mechanical models can contribute to a better design of self-lubricating ceramic composites.[7]

Godet[8] introduced the concept of "third body" and its role on the tribological behavior of sliding components. Many studies in ceramics have confirmed the presence of a third body and its significant role on the tribological behavior under dry contact conditions.[9–12] Although the presence of a deformable third body can results in low friction and wear,[13] some studies have shown the formation of a transfer layer as well as abrasive third body in a ceramic contact limited their application under unlubricated sliding conditions.[14,15] Furthermore, several tribological studies showed an influence of the countersurface on the behavior of third body.[16,17] Ajayi and Ludema[16] studied wear of ceramics sliding against dissimilar countersurfaces at room temperature. They explain that a transfer film is formed due to the strong reattachment of fine wear debris particles during sliding which may or may not occur on both mating tribopair surfaces. The transfer film may be continuous or in islands and several factors play a role in the formation of the transfer film.

* Corresponding author. Tel.: +31 53489 4325; fax: +31 53489 4784.
E-mail addresses: m.valefi@utwente.nl, mahdiyar59@yahoo.com (M. Valefi).

0955-2219/$ – see front matter © 2012 Elsevier Ltd. All rights reserved.
http://dx.doi.org/10.1016/j.jeurceramsoc.2012.07.025

Yittria stabilized tetragonal zirconia polycrystals (3Y-TZP) possess excellent mechanical properties such as strength and toughness, dimensional and chemical stability and wear resistance. However, it shows poor wear behavior under high temperature and dry sliding contact conditions.[18,19] Several researchers have explored the feasibility of embedding a lubricious oxide into the zirconia matrix.[20–24] Kerkwijk et al.,[20] investigated the influence of different solid lubricants on tribological behavior of zirconia ceramic composites at room temperature and concluded that only CuO improved the frictional and wear behavior of zirconia. Ouyang et al.[21] studied the wear behavior of zirconia composite as a function of temperature. They found that addition of $BaCrO_4$ significantly improves intermediate and high temperature wear resistance of zirconia sliding against alumina when compared to the undoped zirconia ceramics. However, they did not investigate the self-lubricating ability of the zirconia composite when sliding against other countersurface materials.

The room temperature tribological performance of CuO–TZP has been recently studied by Song et al.[25] and they suggested that CuO can contribute to the formation of a tribofilm while the CuO–TZP composite is sliding against an alumina countersurface. The self-lubricating behavior of CuO–TZP composite against the alumina countersurface at high temperatures has also been investigated.[26] At 600 °C and higher temperatures, a smooth copper rich third body layer has been found which is formed at interface by plastic deformation of wear debris and decrease the coefficient of friction. The details of the wear mechanism in CuO–TZP/alumina system has been discussed elsewhere.[26,27] It is not clear whether the self-lubricating performance of CuO–TZP varies with the countersurface materials used. There are only a few studies in which the role of the countersurface on high temperature tribological performance of self-lubricating composites has been investigated.[28,29]

In this research, dry sliding wear tests were carried out at 600 °C in air using different countersurfaces and loads, to investigate the role of countersurface material on the unlubricated sliding behavior of CuO–TZP composite. The wear track and wear scar were examined using SEM/EDS and LSM to understand the involved wear mechanisms when different countersurfaces are used.

2. Experimental details

2.1. Material preparation

Details on processing of CuO–TZP composites are described in an earlier publication.[23] CuO–TZP and Y-TZP discs were sintered at 1500 °C for 8 h and 1400 °C for 2 h with a heating and cooling rate of 2 °C/min, respectively. The sintered discs were polished to a surface roughness (R_a) of <100 nm using a diamond paste. To relieve surface residual stresses due to polishing, all the polished discs were annealed at 850 °C for 2 h. The sintered density was measured using the Archimedes method by immersion in mercury.

2.2. High temperature tribological experiments and characterization

Unlubricated sliding wear tests were performed on a ball-on-disc type high temperature tribometer (CSEM, Neuchatel, Switzerland) at 600 °C in air. Commercial high purity alumina, silicon nitride and zirconia balls (GIMEX Technische Keramiek B.V., Geldermalsen, The Netherlands) of 10 mm in diameter were used as countersurfaces. Prior to the sliding tests, both the ball and disc were ultrasonically cleaned with isopropanol alcohol and rinsed with deionized water and then oven dried at 120 °C for 24 h. All wear tests were performed at 600 °C with 1, 2.5 and 5 N loads, a velocity of 0.05 m/s, a radius of the wear track of 10–12 mm, and a sliding distance of 1 km. After the sliding tests, the surfaces of both the ball and disc were examined by a confocal or interference microscope. The wear volume of the discs was determined from wear track profiles obtained using confocal microscope. The wear volume was calculated from the measured wear track width and depth. The worn surface obtained at low load of 1 N was also analyzed with interference microscopy for comparison. The volume loss calculated was then normalized by dividing by the applied load and the sliding distance to obtain the specific wear rate (k).

The Vickers hardness of the disc and ball materials was determined by a micro-indentation test at a load of 10 N and an indentation time of 10 s. Ten indentations were made and the average was used as the hardness. The fracture toughness was obtained using an indentation-strength method using the formula given by Anstis et al.[30] More details about fracture toughness measurements can be found in our previous work.[27] Some of the physical and mechanical properties of the materials used in this study are listed in Table 1.

The worn surfaces were examined using a scanning electron microscope (JEOL, JSM6400 and JCM5000, Japan) equipped with energy dispersive spectrometer (EDS) and a laser scanning microscope (LSM) (Keyence VK-9700K, Japan).

3. Results

3.1. Friction and wear data of CuO–TZP sliding against different countersurfaces

The coefficient of friction (COF) data for undoped TZP and doped CuO–TZP are compared in Table 2, for different applied loads. With increasing load, the COF increased slightly when alumina and zirconia countersurfaces were used, while Si_3N_4 did not show any increase. All countersurfaces showed a reduction in COF when tested against CuO–TZP discs as compared to undoped TZP. The highest reduction was seen with alumina. It is clear from this table that the mean steady state COF for CuO–TZP/Si_3N_4 tribopair at all loads is the highest whereas CuO–TZP/alumina and CuO–TZP/zirconia tribopairs show relatively lower COF values under similar test conditions. At a load of 1 N, the COF for CuO–TZP/alumina is the lowest and for CuO–TZP/zirconia lies in between CuO–TZP/alumina and CuO–TZP/Si_3N_4. However, at higher loads of 2.5 N and 5 N, the

Please cite this article in press as: Valefi M, et al. Influence of countersurface materials on dry sliding performance of CuO/Y-TZP composite at 600 °C. *J Eur Ceram Soc* (2012), http://dx.doi.org/10.1016/j.jeurceramsoc.2012.07.025

Table 1
Physical and mechanical properties of the counterface materials and CuO–TZP disc material.

Properties	Al_2O_3 ball[26]	Si_3N_4 ball	ZrO_2 ball	CuO–TZP disc[26]
Density (g/cm^3)	3.96	3.18	5.84	5.81
H_V (GPa)	20 ± 0.8	17.3 ± 0.4	12.7 ± 0.1	9.5 ± 0.5
E (GPa)	320	310	210	205
CLA surface roughness (nm)	15	15	25	25
Fracture toughness (MPa m$^{1/2}$)	3.4 ± 0.4	5 ± 0.5	4.2 ± 0.2	3.5 ± 0.2
Thermal conductivity (W m K^{-1})	13	20	2.2	3.4

COF for CuO–TZP/alumina and CuO–TZP/zirconia tribopairs are nearly the same.

The specific wear rate (k) of the different tribopairs are shown in Table 3 which also lists initial maximum Hertzian pressure (p_{max}), flash temperature (T_f) and tensile stresses (σ_{max}). The CuO–TZP disc shows very small specific wear rates when sliding against alumina and zirconia countersurfaces at $F = 1$ N (Table 3). However, at same load the specific wear rate of CuO–TZP when in contact with Si_3N_4 is about 2–3 orders of magnitude higher. These data clearly suggest that the countersurface material plays a significant role. With increasing load, the wear rate in CuO–TZP discs increases in all cases, with Si_3N_4 as countersurface exhibiting the least and zirconia the highest increases. Additionally, the specific wear rate data indicate a mild to severe transition with applied load, when CuO–TZP is sliding against alumina and zirconia countersurface balls. This transition with increasing load is consistent with observations in literature on wear of ceramics.[19,24,31–33]

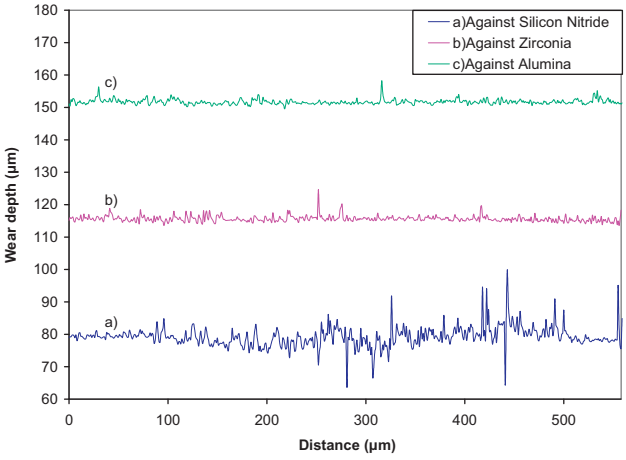

Fig. 1. 2D surface profile of wear tracks, as acquired using confocal LSM (a) against silicon nitride, (b) against zirconia, and (c) against alumina ($F = 1$ N, $v = 0.05$ m/s, and $T = 600$ °C).

3.2. Observation of worn surfaces at low loads

Fig. 1 shows the wear track profiles of CuO–TZP sliding against different countersurfaces at $F = 1$ N obtained using confocal LSM. It is clear that CuO–TZP becomes relatively rough when sliding against Si_3N_4, whereas sliding against zirconia and alumina as countersurfaces results in relatively smooth surfaces. This observation confirms the highest COF measured for CuO–TZP/Si_3N_4 tribopair (Table 2).

The wear tracks and unworn surface of CuO–TZP sliding against different countersurfaces at $F = 1$ N, 600 °C were examined using SEM. Compared to unworn surface, the worn surface of CuO–TZP sliding against Si_3N_4 shows a rough feature indicating a severe wear phenomena. In contrast, CuO–TZP reveals a relatively smooth surface when it is sliding against zirconia. A similar observation has been recently reported for CuO–TZP/alumina by authors.[26] Micrograph 2a indicates lines due to polishing and porosity on the unworn surface. Fig. 2b indicates that microfracture as well as spalling and fragmentation of grains occur on the surface of CuO–TZP sliding against Si_3N_4. CuO–TZP wear tracks sliding against zirconia and alumina appear smooth indicating formation of a smooth thin film as well as plastic deformation of the surface layer (Fig. 2c and d). Although both these tracks appear smooth, CuO–TZP/alumina tribopair indicate presence of submicron wear particles entrapped in the pores (Fig. 2d) while CuO–TZP/zirconia did not (Fig. 2c).

Fig. 3 illustrates the worn surfaces of different countersurface materials after sliding against CuO–TZP at $T = 600$ °C and at different applied loads. The following features are observed when comparing the worn surfaces of the different countersurfaces tested at a low load of 1 N. During sliding, debris from the CuO–TZP disc is transferred and adhered to the Si_3N_4 countersurface contact interface which makes the wear scar surface

Table 2
Coefficient of friction (COF) for undoped and CuO doped TZP discs tested at different applied loads with different counterface materials($T = 600$ °C and $v = 0.05$ m/s).

Disc	Y-TZP			CuO–TZP			Reduction in COF due to CuO (%)		
Counterface	1 N	2.5 N	5 N	1 N	2.5 N	5 N	1 N	2.5 N	5 N
Alumina[a]	0.7 ± 0.03	0.78 ± 0.01	0.79 ± 0.01	0.35 ± 0.05	0.53 ± 0.01	0.56 ± 0.01	50	32	29
Zirconia	0.79 ± 0.02	0.8 ± 0.02	0.82 ± 0.02	0.44 ± 0.04	0.54 ± 0.01	0.54 ± 0.02	44	32	35
Si_3N_4	0.76 ± 0.02	0.7 ± 0.02	0.75 ± 0.01	0.65 ± 0.04	0.69 ± 0.02	0.65 ± 0.04	14	1	13

[a] Data taken from Valefi et al.[26]

Please cite this article in press as: Valefi M, et al. Influence of countersurface materials on dry sliding performance of CuO/Y-TZP composite at 600 °C. *J Eur Ceram Soc* (2012), http://dx.doi.org/10.1016/j.jeurceramsoc.2012.07.025

Table 3
Maximum Hertzian contact pressure (p_{max}), flash temperature (T_f), tensile stresses (σ_{max}) and specific wear rate (k) data for CuO–TZP discs sliding against balls of different countersurface materials at $T = 600\,^{\circ}C$.

Countersurface material	F (N)	p_{max} (GPa)	T_f (°C)	Tensile stress (σ_{max}) (GPa)	k ($\times 10^{-6}$) (mm^3 N^{-1} m^{-1})
Alumina	1	0.52	695	0.37	0.4 ± 0.005
	2.5	0.71	743	0.73	305 ± 15
	5	0.89	751	0.96	390 ± 5
Si_3N_4	1	0.54	725	0.665	19.2 ± 1
	2.5	0.74	732	0.96	22.8 ± 2
	5	0.93	732	1.15	91.5 ± 5
Zirconia	1	0.47	930	0.41	0.6 ± 0.002
	2.5	0.63	1051	0.66	330 ± 20
	5	0.8	1034	0.82	1080 ± 40

appear rough (Fig. 3a). However, the wear scars on zirconia (Fig. 3d) and alumina (Fig. 3g) countersurface balls appear flat, relatively smaller in diameter and the wear debris are piled up at the leading edge of countersurface wear scar. This suggests that a smooth layer is formed at the interface and sheared in further sliding which is accumulated at the leading edge of countersurface contact area. The wear scar diameter of the alumina countersurface was smaller than the other two. An analysis of the wear tracks and wear scar dimensions using the confocal LSM also indicated a smaller dimension for the alumina countersurface.

To evaluate the wear of different countersurface balls against CuO–TZP, wear scar diameter as well as specific wear rate of worn balls were measured and presented in Table 4. Although alumina and zirconia countersurfaces show mild wear ($k < 10^{-6}$) when sliding against CuO–TZP at $F = 1$ N, with Si_3N_4 a higher specific wear rate of two orders of magnitude is obtained.

Table 4
Scar diameter (D) and specific wear rate (k) of different counterface balls sliding against CuO–TZP discs at $T = 600\,^{\circ}C$ with an applied load of 1 N and $v = 0.05$ m/s.

Counterface material	D_{scar} (μm)	k ($\times 10^{-6}$) (mm^3 N^{-1} m^{-1})
Si_3N_4	800 ± 20	4
ZrO_2	350 ± 20	0.15
Al_2O_3	200 ± 30	0.027

In order to find out the composition of the transferred material on the countersurfaces, EDS analyses were performed. Fig. 4 shows the elemental compositional maps of the transfer layer on

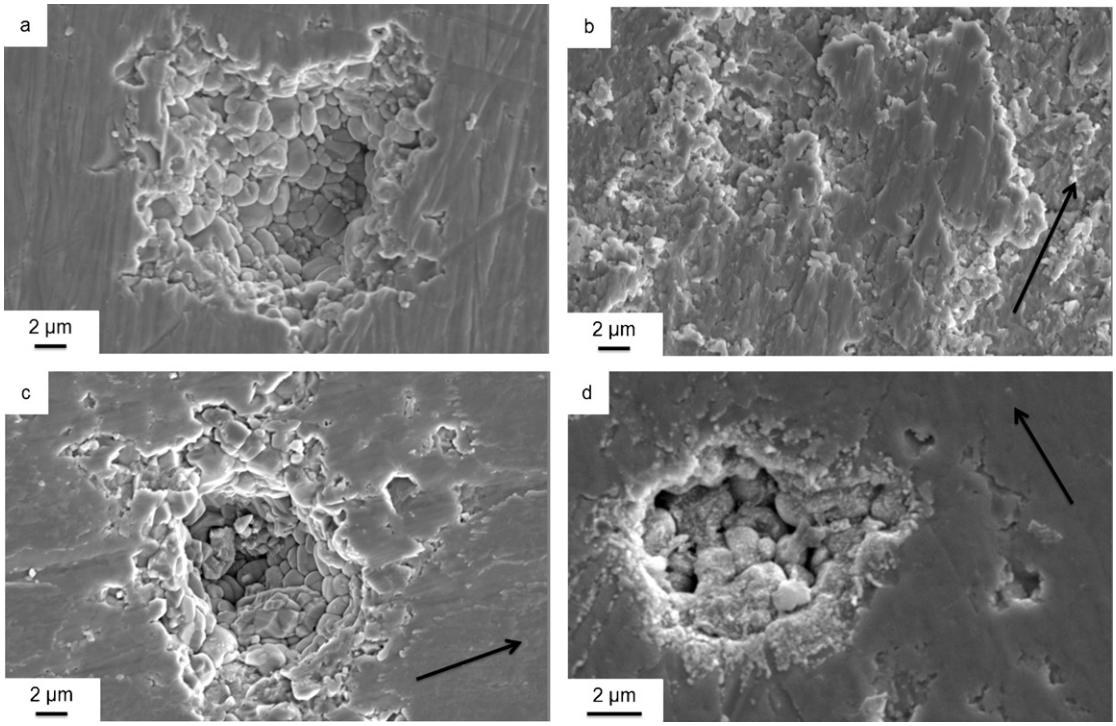

Fig. 2. Higher magnification SEM micrographs of CuO–TZP (a) unworn surface and worn surfaces after sliding against, (b) Si_3N_4, (c) zirconia and (d) alumina ($F = 1$ N, $T = 600\,^{\circ}C$ and $v = 0.05$ m/s) arrows show the sliding direction.

Please cite this article in press as: Valefi M, et al. Influence of countersurface materials on dry sliding performance of CuO/Y-TZP composite at 600 °C. *J Eur Ceram Soc* (2012), http://dx.doi.org/10.1016/j.jeurceramsoc.2012.07.025

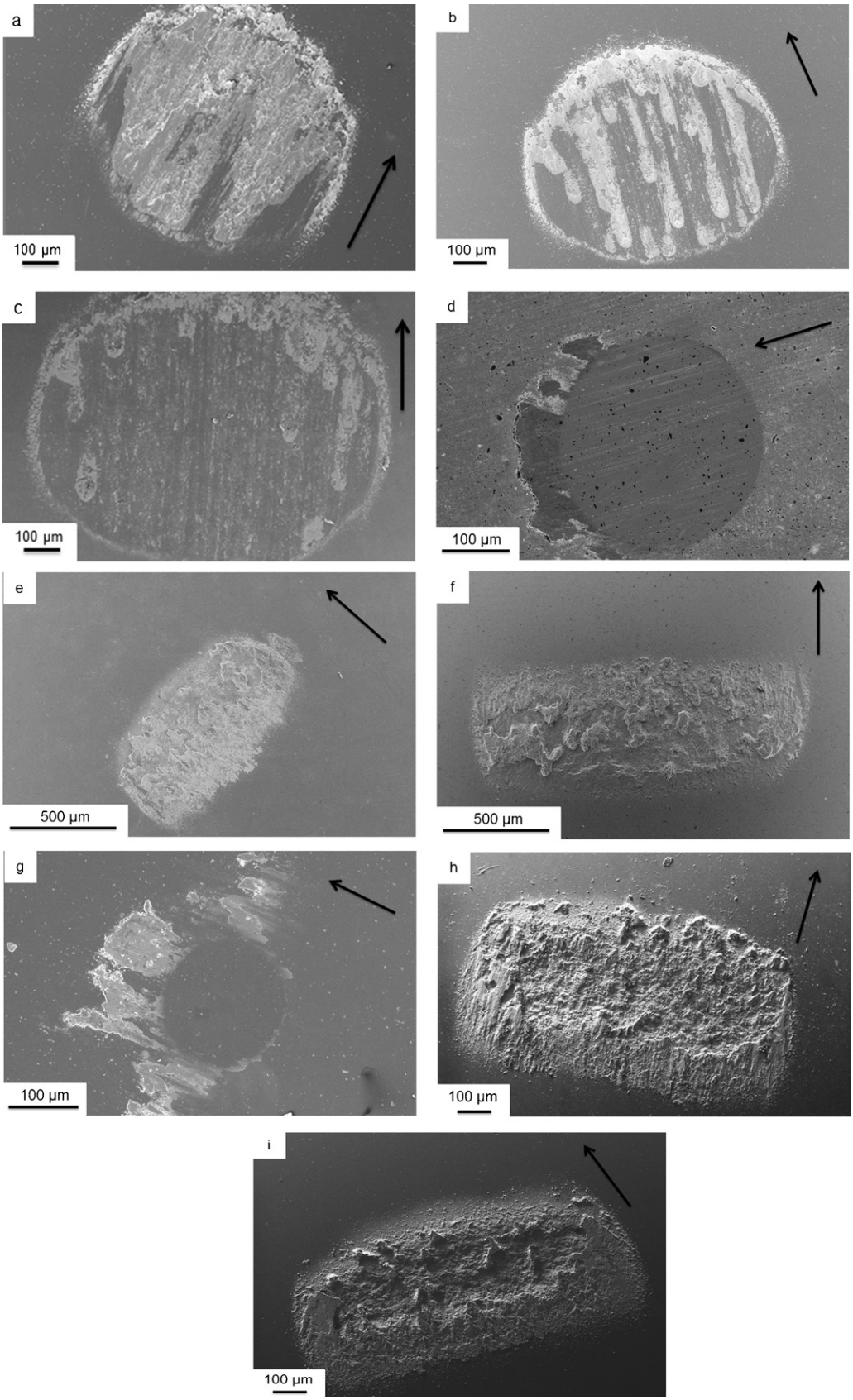

Fig. 3. SEM micrographs of different countersurfaces sliding against CuO–TZP at different loads ($T = 600\,^{\circ}C$ and $v = 0.05$ m/s); Si_3N_4: (a) 1 N, (b) 2.5 N, (c) 5 N; zirconia, (d) 1 N, (e) 2.5 N, (f) 5 N; alumina, (g) 1 N,[26] (h) 2.5 N, and (i) 5 N (arrows show the sliding direction).

Please cite this article in press as: Valefi M, et al. Influence of countersurface materials on dry sliding performance of CuO/Y-TZP composite at 600 °C. *J Eur Ceram Soc* (2012), http://dx.doi.org/10.1016/j.jeurceramsoc.2012.07.025

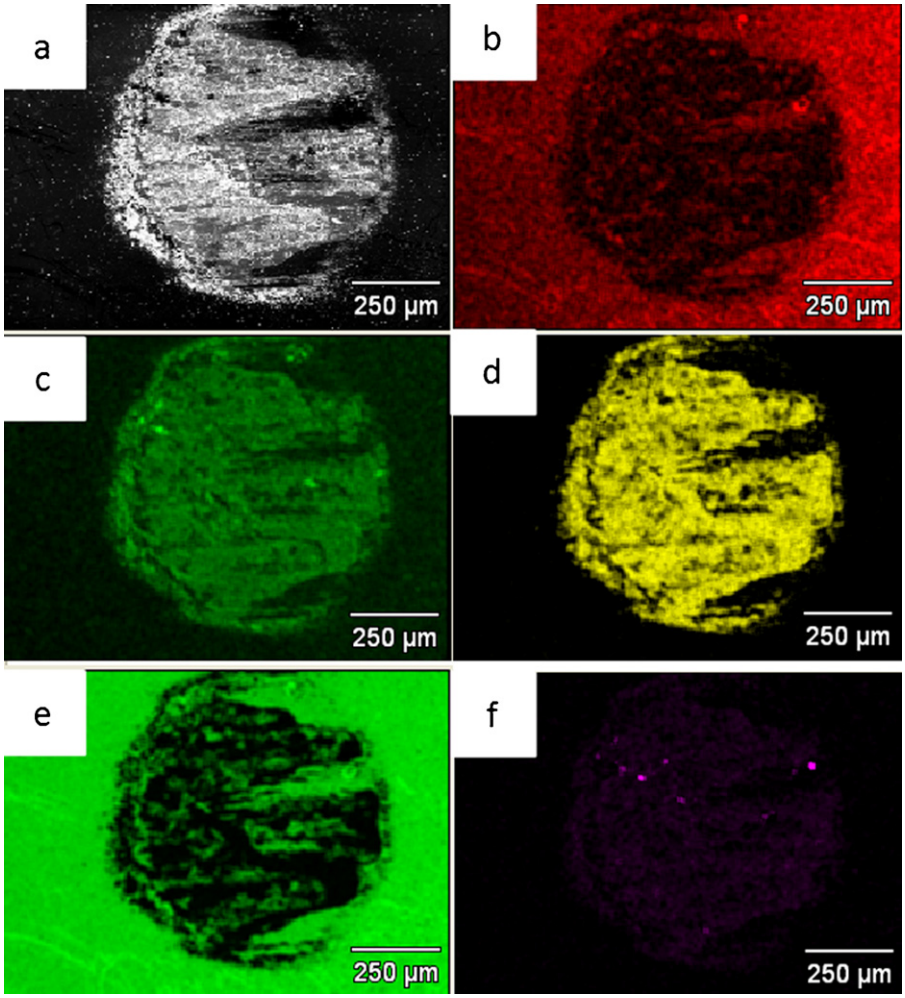

Fig. 4. EDS composition analysis of wear scar on Si_3N_4 ball sliding against CuO–TZP disc at $T = 600\,^{\circ}C$, $F = 1$ N and $v = 0.05$ m/s; (a) backscatter SEM image of EDS-mapped area, (b) Si distribution, (c) O distribution, (d) Zr distribution, (e) N distribution, and (f) Cu distribution.

the Si_3N_4 countersurface sliding against CuO–TZP at $F = 1$ N. The results indicate zirconia transfer to the Si_3N_4 countersurface. Fig. 5 shows the EDS analysis performed on the zirconia countersurface ball after sliding against the CuO–TZP disc at $T = 600\,^{\circ}C$, $F = 1$ N. The transfer layer adhering to the edge of wear scar primarily consists of copper. There is no zirconium found in the transfer layer. A similar observation was made when analyzing the wear scar on the alumina countersurface ball, wherein the transfer layer consisted of copper with zirconium being absent.[26]

3.3. Observation of worn surfaces at higher loads

Fig. 3 shows also the SEM images of the worn surfaces of the different countersurface balls tested at applied loads of 2.5 N and 5 N. In case of Si_3N_4 with increasing load the wear scar size also increased and the shape was elliptical (Fig. 3b and c). However, the amount of adhered zirconia, transferred from the CuO–TZP disc, decreased and a slight pile up of debris at the leading edge was seen. This transfer layer became less stable and adherent to the countersurface as the load is increased. As discussed earlier, both alumina and zirconia show a smooth wear scar when the applied load is 1 N. However, when the load is increased ($F > 1$ N), both countersurfaces became rough and the wear scar is more rectangular than elliptical (Fig. 3e, f, h and i). The zirconia countersurface was worn the most at higher loads. In order to examine the composition of the transfer layer at a higher load of 5 N, EDS analysis was performed on the Si_3N_4 countersurface wear scar after coating with gold (Fig. 6). Both regions with and without the transfer layer were analyzed (Fig. 6a). The EDS spectra (Fig. 6b) clearly indicate that the transfer material consists of Cu and Zr originating from the disc.

SEM micrographs of the wear tracks on CuO–TZP discs sliding against Si_3N_4 and zirconia countersurfaces at $600\,^{\circ}C$ and $F = 5$ N are shown in Fig. 7. The results of wear track produced by alumina countersurface are shown in our earlier publication.[26] These micrographs clearly indicate that third body abrasive wear as well as microfracture are dominant material removal mechanisms for the CuO–TZP disc when it is sliding against all countersurfaces at a high load of 5 N.

Please cite this article in press as: Valefi M, et al. Influence of countersurface materials on dry sliding performance of CuO/Y-TZP composite at 600 °C. *J Eur Ceram Soc* (2012), http://dx.doi.org/10.1016/j.jeurceramsoc.2012.07.025

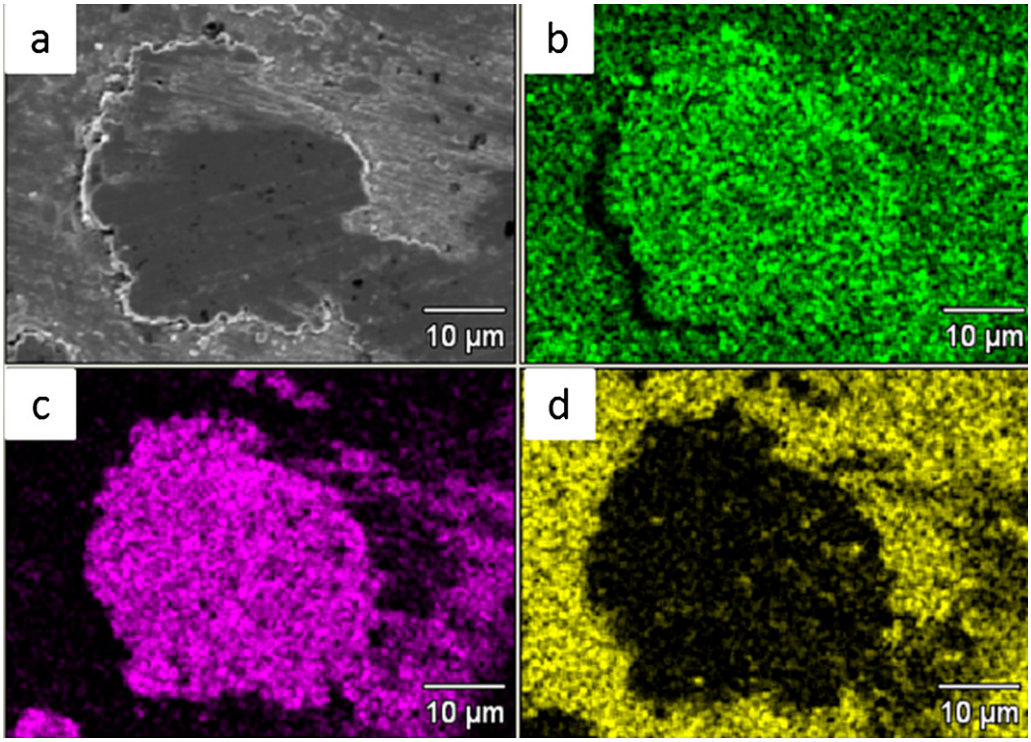

Fig. 5. EDS composition analysis of the transfer layer on zirconia ball sliding against CuO–TZP at $T = 600\,^{\circ}C$, $F = 1$ N and $v = 0.05$ m/s; (a) backscatter SEM image of EDS-mapped area, (b) O distribution, (c) Cu distribution, and (d) Zr distribution.

4. Discussion

The results presented in this study clearly indicate the feasibility of CuO–TZP self-lubrication, which can be controlled by the choice of the countersurface. It is well known that a proper selection of countersurface for a specific tribological condition is crucial.[29,34] The key feature in obtaining self-lubrication is the formation of a lubricious stable third body. The third body formation and its performance appear to depend on countersurface materials as well as contact conditions. Further, it is important to recognize when a mild to severe wear transition will occur when different countersurfaces are used.

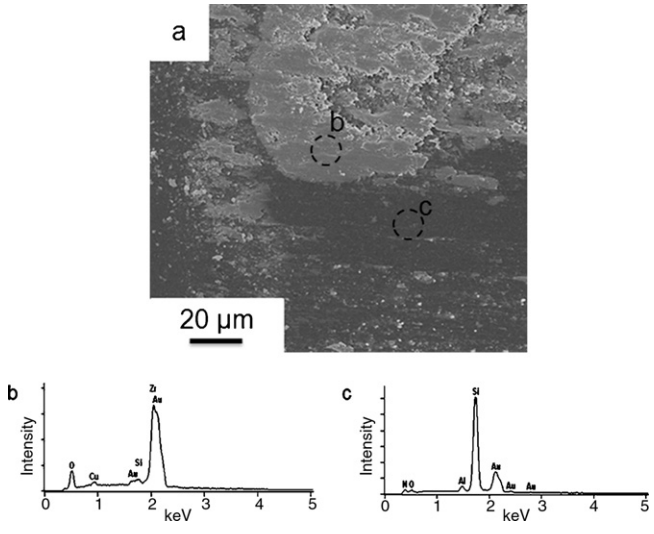

Fig. 6. SEM/EDS analysis of silicon nitride sliding against CuO–TZP at $T = 600\,^{\circ}C$, $F = 5$ N and $v = 0.05$ m/s; (a) wear scar at higher magnification indicating regions chosen for EDS analyses, EDS spectra of (b) transferred material (left) and (c) Si_3N_4 (right).

4.1. Wear mechanism

The Si_3N_4 countersurface behaves quite differently than alumina or zirconia countersurfaces when sliding against CuO–TZP at 1 N load. It is worth recalling our earlier results of alumina countersurface sliding against Y-TZP and CuO–TZP (Fig. 6 of Ref.[26]) at similar test conditions of $F = 1$ N, $T = 595\,^{\circ}C$, wherein the countersurface had a smooth wear scar when sliding against CuO–TZP and a very rough surface when sliding against Y-TZP. Addition of CuO reduced the COF by almost 50% (Table 2). A copper rich third body layer is formed at the contact interface, sheared and transferred to alumina (Fig. 7 of Ref.[26]) or zirconia (Fig. 5) countersurfaces. The mechanism of formation of copper rich layer at the contact interface has been detailed and presented schematically (Figure 12 in[26]) in our previous publications.[26,27] This layer provides lubrication and reduces the COF (Table 2) and specific wear rate (Table 3). It has also been shown that formation of copper rich layer at the contact interface depends on the contact condition such as load and temperature. Above 1 N load the copper rich layer is unstable and the dominant wear mechanisms are abrasive wear and delamination of CuO–TZP sliding against alumina.[26] Such a copper rich layer is not formed on the wear track even at 1 N load while a Si_3N_4 countersurface is sliding against CuO–TZP as revealed by the EDS analysis (Fig. 4). Instead, zirconia is transferred from the CuO–TZP disc

Please cite this article in press as: Valefi M, et al. Influence of countersurface materials on dry sliding performance of CuO/Y-TZP composite at 600 °C. *J Eur Ceram Soc* (2012), http://dx.doi.org/10.1016/j.jeurceramsoc.2012.07.025

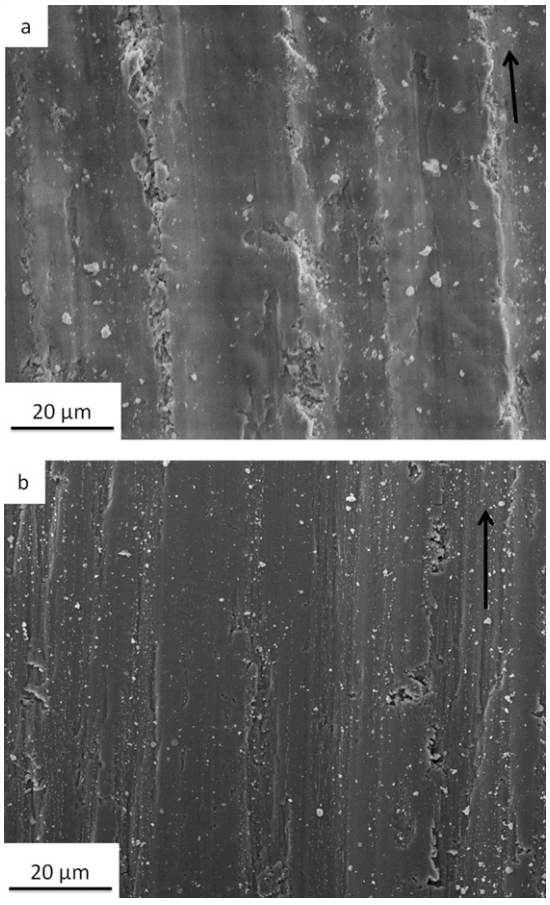

Fig. 7. SEM micrographs of CuO–TZP disc sliding against (a) Si_3N_4 and (b) zirconia; $F = 5$ N, $T = 600$ °C and $v = 0.05$ m/s (arrows show the sliding direction).

to the contact region and adheres to the Si_3N_4 countersurface. This results in higher COF and wear due to increase in surface roughness of the tribopair. During the sliding process, this layer repeatedly appears to break and build again. This is evident from the COF versus sliding distance plots, which showed gradual shallow peaks (Fig. 8, plot a). The confocal LSM analyses of the wear track (Table 3) and wear scar (Table 4) dimensions

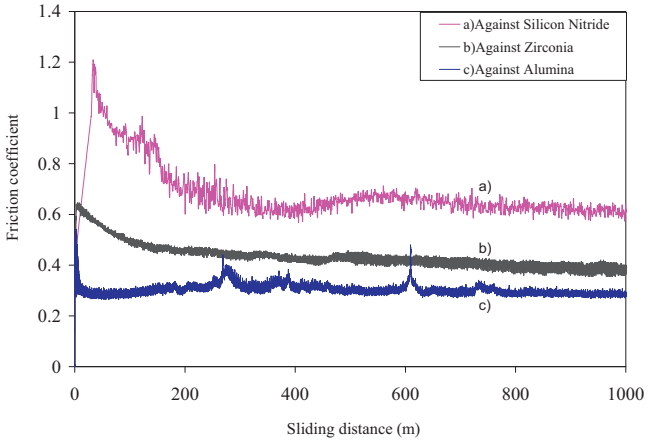

Fig. 8. COF versus sliding distance plots of CuO–TZP disc sliding against (a) Si_3N_4, (b) zirconia and (c) alumina as countersurfaces at 600 °C, $F = 1$ N and $v = 0.05$ m/s.

and SEM micrographs (Fig. 3a, d, and g) indicate that the wear in CuO–TZP/Si_3N_4 tribopair was larger than in the other two tribopairs at a load of 1 N.

According to Fig. 8, at 1 N load Si_3N_4/CuO–TZP tribopair shows the highest initial and steady state COF. The higher COF results in an increase of the maximum principal tensile stress (σ_{max}) at the contact surface, which enhances crack formation and wear debris formation. The maximum tensile stresses at the contact interface imposed by friction are calculated as follows[35]:

$$\sigma_{max} = \left(\frac{6P}{R^2}\right)^{1/3} \left(\frac{1-\nu_1^2}{E_1} + \frac{1-\nu_2^2}{E_2}\right)^{-2/3} \times \left[\frac{1-2\nu_2}{3} + \frac{4+\nu_2}{8}\pi\mu\right] \quad (1)$$

whereas subscript 1 represents the ball and subscript 2 represents the disc, P is the applied load, E is Young's modulus, ν Poisson ratio, R is the radius of the ball and μ the coefficient of friction. The values of tensile stresses are given in Table 3. The tensile stresses are 1.6–1.8 times higher when Si_3N_4 is used as countersurface compared to zirconia or alumina. In addition, the initial tensile stresses are much higher for CuO–TZP/Si_3N_4 tribopair according to Fig. 8. Based on the calculated tensile stresses (Table 3) and the formation of zirconia transfer layer (Fig. 4), it is most likely that more zirconia debris are formed in addition to copper rich phase, in case of Si_3N_4 at the early stage. A short sliding distance test (7 m) was performed with both alumina and Si_3N_4 countersurfaces, before reaching to a steady state COF. The EDS analysis (the results are not shown here) on the accumulated debris ahead of Si_3N_4 countersurface contained mostly zirconium. On the other hand, wear debris ahead of alumina countersurface found to be copper rich. These results suggest that in the case of Si_3N_4 countersurface, fine wear debris which contains more zirconia are compacted at the interface, shear and adhere to countersurface (Fig. 4) under favorable contact conditions of high temperature and contact pressure. Therefore, a stable copper rich third body could not be formed and the resulting third body mainly consisted of zirconia.

Ajayi and Ludema[16] showed that an oxide layer will adhere to another oxide surface rather than on to a non-oxide surface. However, our observation indicates that zirconia adheres to Si_3N_4 countersurface. It has been reported in literature that triboxidation of Si_3N_4 tribopair is most likely at the sliding interface under different test conditions.[36–39] In all these studies, EDS technique has been employed in the elemental composition analyses. All suggest the formation of silicon oxide as a possibility only, from somewhat a higher oxygen content observed on a surface layer. In order to study the interaction of Si_3N_4 with zirconia and possible oxidation of Si_3N_4, different analysis methods such as XRD, SEM/EDS, Raman spectroscopy as well as micro-FTIR were performed on the wear debris, wear tracks of CuO–TZP and Si_3N_4 countersurface. We could not detect the presence of silica from the analysis of wear debris using XRD. XRD and Raman spectroscopy analyses on debris reveal only the presence of zirconia. These observations suggest that the amount of silica phase if at all present, is below detection limit of these

Please cite this article in press as: Valefi M, et al. Influence of countersurface materials on dry sliding performance of CuO/Y-TZP composite at 600 °C. *J Eur Ceram Soc* (2012), http://dx.doi.org/10.1016/j.jeurceramsoc.2012.07.025

analyzes. Further, micro-FTIR analysis on the unworn and the worn scar of Si_3N_4 ball did not indicate any formation of any Si–O bond. According to EDS analysis results shown in Fig. 6b and c, oxygen peak is present on the worn scar of Si_3N_4. As expected, the peak intensity is relatively higher from zirconia transfer layer (Fig. 6b) as compared intensity from a region free of such a layer (Fig. 6c), both locations being within the wear scar (Fig. 6a). However, transfer of zirconia to Si_3N_4 makes it impossible to detect oxygen peak corresponding to silicon oxide alone. On the other hand, the possibility of silica formation cannot be ruled out due to a high contact temperature (Table 3) and the presence of oxygen rich zirconia at the contact area. It has been shown that in the self-mated Si_3N_4 when the temperature is increased above 300 °C, the oxidation rate of Si_3N_4 is enhanced with increase in temperature at the contact surface.[39] Based on the calculated flash temperature (Table 3), a partial oxidation of Si_3N_4 is likely to occur at the contact interface. The formed silica layer will be soft due to high temperature at the interface and can easily embed zirconia debris. This will increase the surface roughness of countersurface resulting in highest COF as shown in Fig. 8. Presence of silica at the interface will facilitate adherence of zirconia to the Si_3N_4 countersurface which is in agreement with observation in literature that oxide to oxide contact can form more coherent and stable transfer layer.[16] However, when the contact stresses are high, the transfer film may be broken due to its limited load-bearing ability. It is not clear why CuO debris do not stick to the presumed silica layer formed on the Si_3N_4 countersurface and produce a copper rich third body as seen with zirconia and alumina countersurfaces. In Fig. 9, an attempt has been made to illustrate the above wear mechanism.

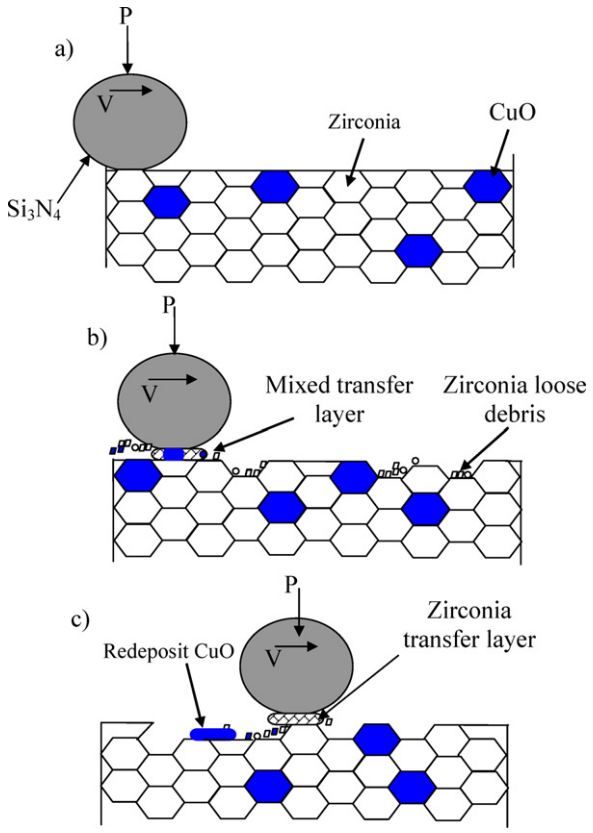

Fig. 9. Schematic representation of the wear mechanism of CuO–TZP composite in different stage of sliding process against Si_3N_4.

4.2. Mild and severe regimes

Though this work in primarily focused on studying the mild wear regime, wear tests have also been conducted at severe conditions. The SEM micrographs of wear scars of the countersurfaces (Fig. 3) and the wear tracks (Fig. 7) indicate that the wear in CuO–TZP/Si_3N_4 tribopair is different. At higher loads of 2.5 N and 5 N, the wear scars (Fig. 3b and c) are elliptical and contain islands of transfer layer of zirconia while the wear tracks (Fig. 7b) show deep grooves probably caused by the ploughing action of the wear debris at the contact interface. The surfaces of zirconia (Fig. 3e and f) and alumina (Fig. 3h and i) countersurfaces indicate the wear scar to be rectangular shaped with the short side lying along the sliding direction and a very rough morphology. Under these circumstances, debris act as an abrasive third body and result in an increase in wear rate. In these cases, the lubrication effect of copper oxide rich third body will be overwhelmed by the abrasive action of the harder debris.

According to Table 3, the specific wear rate increased as the load is increased for all the countersurfaces. This is consistent with results quoted in literature.[31,32,40] It is clear from the specific wear rate data that CuO–TZP shows the highest specific wear rate at 5 N against zirconia and a significantly lower wear rate against Si_3N_4. The low thermal conductivity of zirconia (Table 1) results in a higher flash temperature as compared to the other countersurfaces (Table 3). As a result of higher flash temperature, more thermal stresses are imposed to the sliding surface. The combinations of mechanical and thermal stresses will generate more wear debris, which will act as an abrasive third body.

Based on results of this study, tribological performance of CuO–TZP systems can be altered by choice of countersurface used. Fig. 10 shows the wear mode of CuO–TZP composite sliding against different countersurfaces at 600 °C with different contact loads. It is well known that a transition from mild to severe takes place for ceramics when the specific wear rate

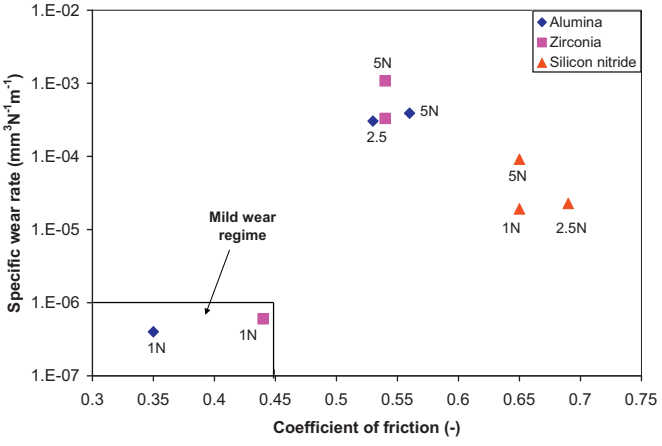

Fig. 10. Wear transition diagram of CuO–TZP composite sliding against different countersurfaces (T = 600 °C and v = 0.05 m/s).

Please cite this article in press as: Valefi M, et al. Influence of countersurface materials on dry sliding performance of CuO/Y-TZP composite at 600 °C. *J Eur Ceram Soc* (2012), http://dx.doi.org/10.1016/j.jeurceramsoc.2012.07.025

value is more than 10^{-6}.[31] In this figure, the solid line indicates the transition from mild to severe. It is clear from this figure that CuO–TZP shows mild and severe wear depending on tribological conditions. In mild wear regime, the wear mechanism is dominated by the self-lubricating ability of this composite. This results in low COF and less wear in case of alumina and zirconia countersurfaces. However, the lack of a lubricant layer results in severe wear when Si_3N_4 countersurface is used. All the countersurfaces result in severe wear as the contact load is increased. The selection of countersurface should be such that a lubricious third body forms between the contacting bodies and protect the materials from severe wear.

5. Conclusions

In the present study to evaluate dry sliding wear performance of CuO–TZP at 600 °C using a ball on disc test configuration, the results indicate that addition of CuO to TZP reduces the COF for different countersurfaces. Alumina and zirconia countersurfaces showed a mild to severe wear transition as the load is increased. For mild wear sliding contact applications using CuO–TZP at 600 °C, both alumina and zirconia countersurfaces are suitable as they show low COF and specific wear rates ($k < 10^{-6}$). Si_3N_4 is unsuitable as countersurface material for sliding against CuO–TZP due to transfer of zirconia and lack of presence of copper rich third body at the sliding interface. Alumina may perform marginally better than zirconia as countersurface material. For a stable lubricious third body formation, both countersurface and disc material must be compatible with the chosen solid lubricant.

Acknowledgments

The authors thank L. Vargas, W. Lette and T. Bor for assistance with SEM, confocal microscopy and XRD measurements, respectively. L. Winnubst and Inorganic membrane group at University of Twente are appreciated for providing experimental facilities needed to fabricate the composite disc material. Funding of this work was provided by the Dutch Governmental Program “IOP Self Healing Materials”.

References

1. Dowson D. *History of tribology*. Professional Engineering Publishing; 1998.
2. Perez R. Carbon nanotubes: not that slippery. *Nat Mater* 2009;**8**(11):857–8.
3. Gangopadhyay A, Jahanmir S, Peterson MB. Self-lubricating ceramic matrix composites. In: Jahanimr S, editor. *Friction and wear of ceramics*. Marcel Dekker; 1994.
4. Jin Y, Kato K, Umehara N. Tribological properties of self-lubricating CMC/Al_2O_3 pairs at high temperature in air. *Tribol Lett* 1998;**4**(3):243–50.
5. Zhou Z, Rainforth WM, Luo Q, Hovsepian PE, Ojeda JJ, Romero-Gonzalez ME. Wear and friction of TiAlN/VN coatings against Al_2O_3 in air at room and elevated temperatures. *Acta Mater* 2010;**58**(8):2912–25.
6. Jianxin D, Tongkun C, Lili L. Self-lubricating behaviors of Al_2O_3/TiB_2 ceramic tools in dry high-speed machining of hardened steel. *J Eur Ceram Soc* 2005;**25**(7):1073–9.
7. Song J, Valefi M, de Rooij M, Schipper DJ. A mechanical model for surface layer formation on self-lubricating ceramic composites. *Wear* 2010;**268**(9–10):1072–9.
8. Godet M. The third-body approach: a mechanical view of wear. *Wear* 1984;**100**(1–3):437–52.
9. Denape J, Lamon J. Sliding friction of ceramics: mechanical action of the wear debris. *J Mater Sci* 1990;**25**(8):3592–604.
10. Ravikiran A, Jahanmir S. Effect of interfacial layers on wear behavior of a dental glass–ceramic. *J Am Ceram Soc* 2000;**83**(7):1831–3.
11. Kalin M, Jahanmir S, Drazic G. Wear Mechanisms of glass-infiltrated alumina sliding against alumina in water. *J Am Ceram Soc* 2005;**88**(2):346–52.
12. Khanna R, Basu B. Sliding wear properties of self-mated yttria-stabilized tetragonal zirconia ceramics in cryogenic environment. *J Am Ceram Soc* 2007;**90**(8):2525–34.
13. Singer IL. Mechanics and chemistry of solids in sliding contact. *Langmuir* 1996;**12**(19):4486–91.
14. Andersson P, Holmberg K. Limitations on the use of ceramics in unlubricated sliding applications due to transfer layer formation. *Wear* 1994;**175**(1–2):1–8.
15. Hsu SM, Shen M. Wear prediction of ceramics. *Wear* 2004;**256**(9–10):867–78.
16. Ajayi OO, Ludema KC. Mechanism of transfer film formation during repeat pass sliding of ceramic materials. *Wear* 1990;**140**(2):191–206.
17. Boch P, Platon F, Kapelski G. Tribological and interfacial phenomena in Al_2O_3/SiC and SiC/SiC couples at high temperature. *J Eur Ceram Soc* 1989;**5**(4):223–8.
18. Scott HG. In: Lumeda KC, editor. *Friction and wear of zirconia at very low sliding speed, wear of materials*. New York: American Society of Mechanical Engineers; 1985. p. 8–12.
19. Woydt M, Kadoori J, Habig KH, Hausner H. Unlubricated sliding behaviour of various zirconia-based ceramics. *J Eur Ceram Soc* 1991;**7**(3):135–45.
20. Kerkwijk B, Garcia M, van Zyl WE, Winnubst L, Mulder EJ, Schipper DJ, Verweij H. Friction behaviour of solid oxide lubricants as second phase in α-Al_2O_3 and stabilised ZrO_2 composites. *Wear* 2004;**256**(1–2):182–9.
21. Ouyang JH, Sasaki S, Murakami T, Umeda K. Spark-plasma-sintered $ZrO_2(Y_2O_3)$-$BaCrO_4$ self-lubricating composites for high temperature tribological applications. *Ceram Int* 2005;**31**(4):543–53.
22. Liu H, Xue Q. The tribological properties of TZP-graphite self-lubricating ceramics. *Wear* 1996;**198**(1–2):143–9.
23. Ran S, Winnubst L, Blank DHA, Pasaribu HR, Sloetjes J-W, Schipper DJ. Effect of microstructure on the tribological and mechanical properties of CuO-doped 3Y-TZP ceramics. *J Am Ceram Soc* 2007;**90**(9):2747–52.
24. Pasaribu HR, Sloetjes JW, Schipper DJ. Friction reduction by adding copper oxide into alumina and zirconia ceramics. *Wear* 2003;**255**(1–6):699–707.
25. Song J, Valefi M, de Rooij M, Schipper DJ, Winnubst L. The effect of alumina countersurface on the friction reduction of CuO/3Y-TZP at room temperature. *Wear* 2012;**274–275**:75–83.
26. Valefi M, de Rooij M, Schipper DJ, Winnubst L. High-temperature tribological and self-lubricating behavior of copper oxide-doped Y-TZP composite sliding against alumina. *J Am Ceram Soc* 2011;**94**(12):4426–34.
27. Valefi M, de Rooij M, Schipper DJ, Winnubst L. Effect of temperature on friction and wear behaviour of CuO–zirconia composites. *J Eur Ceram Soc* 2012;**32**:2235–42.
28. Li JL, Xiong DS. Tribological properties of nickel-based self-lubricating composite at elevated temperature and countersurface material selection. *Wear* 2008;**265**(3–4):533–9.
29. DellaCorte C. The effect of countersurface on the tribological performance of a high temperature solid lubricant composite from 25 to 650 °C. *Surf Coat Technol* 1996;**86–87**:486–92.
30. Anstis G, Chantikul P, Lawn B, Marshall D. A critical evaluation of indentation techniques for measuring fracture toughness: I. Direct crack measurements. *J Am Ceram Soc* 1981;**64**(9):533–8.
31. Kato K, Adachi K. Wear of advanced ceramics. *Wear* 2002;**253**(11–12):1097–104.
32. Dong X, Jahanmir S, Hsu SM. Tribological characteristics of α-alumina at elevated temperatures. *J Am Ceram Soc* 1991;**74**(5):1036–44.
33. Wang Y, Hsu SM. Wear and wear transition mechanisms of ceramics. *Wear* 1996;**195**(1–2):112–22.
34. Zhou F, Adachi K, Kato K. Friction and wear behavior of BCN coatings sliding against ceramic and steel balls in various environments. *Wear* 2006;**261**(3–4):301–10.

Please cite this article in press as: Valefi M, et al. Influence of countersurface materials on dry sliding performance of CuO/Y-TZP composite at 600 °C. *J Eur Ceram Soc* (2012), http://dx.doi.org/10.1016/j.jeurceramsoc.2012.07.025

35. Ajayi OO, Erdemir A, Lee RH, Nichols FA. Sliding wear of silicon carbide–titanium boride–ceramic-matrix composite. *J Am Ceram Soc* 1993;**76**:511–7.
36. Skopp A, Woydt M, Habig K-H. Unlubricated sliding friction and wear of various Si_3N_4 pairs between 22 and 1000 °C. *Tribol Int* 1990;**23**: 189–99.
37. Khader I, Hashibson A, Albina J-M. Wear and corrosion of silicon nitride rolling tools in copper rolling. *Wear* 2011;**271**:2531–41.
38. Waesche R, Hartelt M, Weihnacht V. Influence of counterbody material on wear of ta-C coatings under fretting conditions at elevated temperature. *Wear* 2009;**267**:2208–15.
39. Hadad M, Blugan G, Kubler J, Rosset E, Rohr L, Michler J. Tribological behaviour of Si_3N_4–%TiN based composites and multi-layer laminates. *Wear* 2006;**260**:634–41.
40. Lee SW, Hsu SM, Shen MC. Ceramic wear maps: zirconia. *J Am Ceram Soc* 1993;**76**(8):1937–47.

Please cite this article in press as: Valefi M, et al. Influence of countersurface materials on dry sliding performance of CuO/Y-TZP composite at 600 °C. *J Eur Ceram Soc* (2012), http://dx.doi.org/10.1016/j.jeurceramsoc.2012.07.025